NUMERICAL SIMULATION OF BASIN EFFECTS ON LONG-PERIOD GROUND MOTION

S. M. Day[1], J. Bielak[2], D. Dreger[3], R. Graves[4], S. Larsen[5], K. B. Olsen[1], A. Pitarka[4], and L. Ramirez-Guzman[2]

ABSTRACT

We simulate long-period (0-0.5 Hz) ground motion time histories for a suite of sixty scenario earthquakes (Mw 6.3 to Mw 7.1) within the Los Angeles basin region. Fault geometries are based upon the Southern California (SCEC) Community Fault Model, and 3D seismic velocity structure is based upon the SCEC Community Velocity Model. The ground motion simulations are done using 5 different 3D finite difference and finite element codes, and we perform numerous cross-check calculations to insure consistency among these codes. The nearly 300,000 synthetic time histories from the scenario simulations provide a resource for ground motion estimation and engineering studies of large, long-period structures, or smaller structures undergoing large, nonlinear deformations. By normalizing spectral accelerations to those from simulations performed for reference hard-rock models, we characterize the source-averaged effect of basin depth on spectral acceleration. For this purpose, we use depth (D) to the 1.5 km/s S velocity isosurface as the predictor variable. The resulting mean basin-depth effect is period dependent, and both smoother (as a function of period and depth) and higher in amplitude than predictions from local 1D models. The main requirement for the use of the results in construction of attenuation relationships is determining the extent to which the basin effect, as defined and quantified in this study, is already accounted for implicitly in existing attenuation relationships, through (1) departures of the average "rock" site from our idealized reference model, and (2) correlation of basin depth with other predictor variables (such as Vs_{30}).

Introduction

We apply 3D numerical modeling to improve understanding of the effects of sedimentary basins on long-period ($\geq$ ~2 seconds) earthquake ground motion. The study employs both finite element (FE) and finite difference (FD) methods to compute ground motion from propagating earthquake sources in the Southern California Earthquake Center (SCEC) Community Velocity Model (CVM), a 3D seismic velocity model for southern California (Magistrale et al., 2000).

[1]Dept. of Geological Sciences, San Diego State University, San Diego CA 92182
[2]Dept. of Civil and Environmental Engineering, Carnegie-Mellon University, Pittsburgh PA 15213
[3]Berkeley Seismological Laboratory, University of California, Berkeley, Berkeley CA 94720
[4]URS Corporation, 566 El Dorado Street, Pasadena CA 91101
[5]Lawrence Livermore National Laboratory, Livermore CA 94550

Previous work (Day et al, 2001; 2003) documented the mathematical soundness of the five simulation codes used for the project by comparing results from a set of test simulations. The comparisons show that all five codes are accurate for the class of problems relevant to this study (Day, 2003). These tests also demonstrated the validity of putting a lower threshold on the velocity model to exclude S wave velocity values in the CVM that fall below 500 m/s. The tests confirmed that imposing this threshold (for the sake of computational efficiency) had negligible effects within the target bandwidth of 0-0.5 Hz. Validations of these numerical modeling procedures using recorded strong ground motions for the 1994 Northridge, California, earthquake are reported in Olsen et al. (2003).

For the current investigation, we compute long-period ground motion in the SCEC CVM for a suite of 60 earthquake scenarios. The 3-component ground motion time histories from these scenarios are saved on a grid of 1600 sites covering the Los Angeles region, including sites in the Los Angeles, San Fernando, and San Gabriel basins, as well as rock sites in the intervening areas. The results from the current study take 2 forms: (1) We have saved and archived a library of time histories from the 60 scenarios. In cooperation with the SCEC Community Modeling Environment project, these time histories are available online, through a web interface specialized to engineering applications (http://sceclib.sdsc.edu/LAWeb). These long-period time histories capture basin amplifications, rupture-propagation-induced directivity, and 3D seismic focusing phenomena. They are suitable for the engineering analyses of large, long-period structures, and smaller structures undergoing large, nonlinear deformations. (2) The results of the simulation suite have been analyzed to estimate response spectral amplification effects as a function of basin depth and period. The resulting mean response has been characterized parametrically and provided to the Next Generation Attenuation (NGA) project to guide development of attenuation relations in the empirical (NGA-E) phase of the project.

Earthquake Scenarios

We model sources on ten different faults, or fault configurations (for example, the Puente Hills fault is modeled in 3 different segmentation configurations). For each fault, we simulate 6 sources, using combinations of 3 different static slip distributions and 2 hypocenter locations. These are kinematic simulations: rupture velocity, static slip, and the form of the slip velocity function are all specified *a priori*.

The areal coverage for the 3D models is the 100 km x 100 km region outlined by the green box in Figure 1. In all simulations, the boundaries of the computational domain (i.e. absorbing boundaries) lie at or outside of this area and extend to a depth of at least 30 km. For the uniform grid FD modelers, a grid spacing of 200 m was used. The FE grid uses a variable element size, with near-surface elements as small as 30 m in dimension.

We use the 10 faults listed in Table 1 for the scenario calculations. The surface projections of these faults are also shown in Figure 1. The longitude and latitude coordinates in this table refer to the geographic location of the top center of the fault, that is, the point on the surface that is directly above the midpoint of the top edge of the fault. Strike, dip and rake follows Aki and Richards' (1980) convention. Length, width and depth are all given in km. The depth refers to the depth below the surface of the top edge of the fault (0 corresponding to a

surface-rupturing event).

For each of the fault geometries, we generate 3 random slip distributions, as realizations of a stochastic model, for use in the simulations. The slip distributions are generated following some empirical rules for the size and distribution of asperities as given by Somerville et al. (1999). The slip values on the fault are drawn from a uniformly distributed random variable, then spatially filtered to give a spectral decay inversely proportional to wavenumber squared, with a corner wavenumber at approximately $1/L$, where L is fault length. Finally, the slip values are scaled to the target moment of the scenario. The two hypocenter locations are defined as follows for each fault: Hypocenter 1 is located at an along-strike (AS_1) distance of 0.25 of the fault length and at a down-dip (DD_1) distance of 0.7 of the fault width (measured within the fault plane from the top edge of the fault, not the ground surface). Hypocenter 2 is located at an along strike (AS_2) distance of 0.75 of the fault length and at a down-dip (DD_2) distance of 0.7 of the fault width.

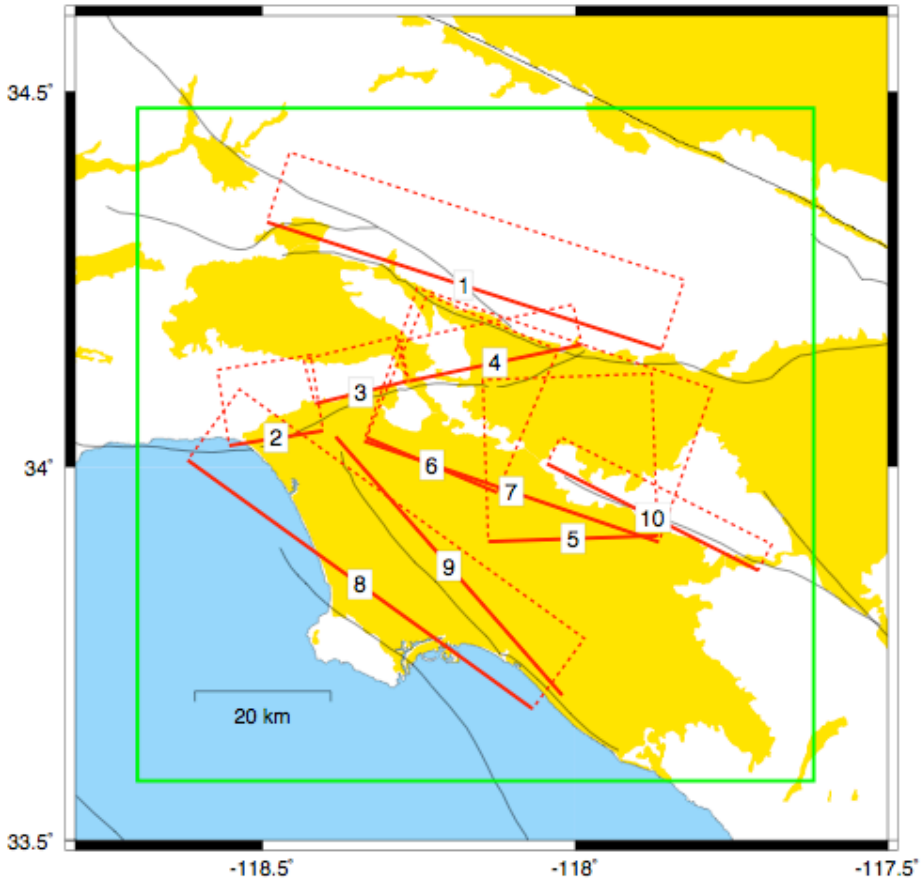

Figure 1. Map of scenario events and model region. See Table 1 for fault names and event magnitudes.

The slip velocity function for each simulation is an isosceles triangle with a base of duration T_r. The value of T_r is magnitude dependent and given by the empirically derived expression (Somerville et al., 1999):

$$\log_{10}(T_r) = 0.5(M_w + 10.7) + \log_{10}(2.0 \times 10^{-9}) , \quad (1)$$

where $\log_{10}$ is base 10 logarithm and M_w is moment magnitude. Rupture velocity is constant for all faults and all slip models. This value is set at 2.8 km/s. The rupture starts at the hypocenter and spreads radially outward from this point at the specified velocity. The simulated duration for each scenario is 80 seconds.

All simulations use the SCEC CVM, Version 2, except for modifications described below to impose a lower limit on the velocities and add anelastic attenuation. The unmodified model is described in Magistrale et al. (2000). The SCEC model is modified as follows: Replace the SCEC model S velocity with the value 500 m/s whenever the SCEC model value falls below 500 m/s. Whenever this minimum *S* velocity is imposed, the *P* wave velocity is set equal to 3 times the S velocity (1500 m/s in this case). Density values follow the SCEC model without modification. The quality factors for *P* and *S* waves, respectively, Q_p and Q_s, are set to the preferred *Q* model of Olsen et al. (2003).

The 3-component time histories are saved on a 2 km x 2 km grid covering the inner 80 km x 80 km portion of the model area. No filtering is applied to the output. The result is 1600 sites (4800 time histories) for each scenario simulation. For all 60 scenarios, and all sites, we compute response spectral acceleration (Sa), for 5% damping, as a function of period, for each component of motion. This is done for 26 periods in the range 2-10 seconds: spectral acceleration is computed at 0.2 second intervals between 2 and 5 second, and at 0.5 second intervals between 5 and 10 seconds.

Table 1. List of Fault Rupture Scenarios

Fault	Lon (TC)	Lat (TC)	M_w	Length	Width	Strike	Dip	Rake	Depth
1) smad	-118.1776	34.2415	7.0	61	18	288	53	90	0
2) smon1	-118.4785	34.0385	6.3	14	14	261	36	45	1
3) hwood	-118.3427	34.0993	6.4	14	19	256	69	70	0
4) raym2	-118.1281	34.1388	6.6	26	17	258	69	70	0
5) ph2e	-118.0037	33.9042	6.8	25	27	268	27	90	3
6) phla	-118.2293	34.0026	6.7	21	26	293	28	90	3
7) phall	-118.1020	33.9670	7.1	46	27	289	27	90	2
8) comp	-118.3440	33.8428	6.9	63	14	306	22	90	5
9) nin	-118.2020	33.8676	6.9	51	16	319	90	180	0
10) whitn	-117.8762	33.9330	6.7	35	15	297	73	160	0

Reference Simulations

To aid us in quantifying the effect of sedimentary basins on the computed ground motions, we perform several auxiliary, or "reference," simulations. For each of the 10 faults, we select one rupture scenario, and repeat that simulation using the same source model, but replacing the SCEC CVM with a horizontally stratified model. The stratified reference model corresponds to an artificially high-velocity, unweathered hard-rock site. This reference velocity model was constructed by laterally extending a vertical profile of the SCEC CVM located at (–118.08333, 34.29167), in the San Gabriel Mountains. As noted, surface *S* velocities are artificially high (3.2 km/s) in the resulting model, since this part of the SCEC model does not

account for a weathered layer. The purpose of the reference simulations is solely to provide a normalization for the results from the simulations done in the full SCEC CMV, as an approximate means of isolating basin effects from source effects.

Response Spectral Amplifications

Basin amplification effects result from interaction of the wavefield with basin margins, and depend in a complex, poorly understood manner on period, source location, source distance, basin geometry, sediment velocity distribution, and site location within the basin. The 60 scenarios provide synthetic data that can be used to improve our understanding of these effects. We take an initial step in this direction by attempting to isolate the effects of period and local basin depth. To isolate these 2 effects, we average over sources. As response spectral values vary much more between ruptures on different faults than between ruptures on a given fault, we have computed averages using only 1 of the 6 scenarios from each fault, giving us a 10-event subset of the simulations. This subset misses a small amount of the variability in basin response present in the full 60-event suite, but allows us to work with spectral values normalized to the reference structure, without requiring 60 reference-structure simulations. Tests using a small number of additional events confirm that source effects have been adequately removed by this procedure.

Method

We first bin the sites according to the local basin depth D at a site, with D_j denoting the depth at site j. For this purpose, we define the depth D to be the depth to the 1.5 km/s S wave velocity isosurface. Note, however, that in the SCEC CVM, the depths of different S velocity isosurfaces are strongly correlated, and therefore very similar results are obtained using the 1.0 or 2.5 km/s isosurface instead of the 1.5 km/s isosurface. The binning is represented through a matrix W. We define N_{bin} bins by specifying depths D_q^{bin}, q=1, . . . N_{bin}, at the bin centers, spaced at equal intervals ΔD (i.e., $D_q^{bin} == (q - 1/2)\Delta D$, and then form W,

$$W_{qj} = \begin{cases} 1 \text{ if } \left(D_q^{bin} - \Delta D/2\right) \le D_j < \left(D_q^{bin} + \Delta D/2\right) \\ 0 \quad \text{otherwise} \end{cases}. \tag{2}$$

For consistency with most empirical attenuation relations, we work with response spectral values averaged over the two horizontal components. For the ith event and jth site, we form the ratio $Sa_{ij}(P_k)/Sa_{ij}^{ref}(P_k)$, where $Sa_{ij}(P_k)$ is the absolute spectral acceleration (averaged over horizontal components) from SCEC-CVM event i at site j and period P_{k}, and $Sa_{ij}^{ref}(P_k)$ is the corresponding quantity for the corresponding reference-model event. Then we form the source-averaged basin response factor $B(D_{\text{q}}, P_{\text{k}})$ by averaging over all N_{site} sites (N_{site}=1600), and over all N_{ev} events, where in this case N_{ev} is 10:

$$B(D_q, P_k) = \left(N_{ev} \sum_{j=1}^{N_{site}} W_{qj} \right)^{-1} \sum_{i=1}^{N_{ev}} \sum_{j=1}^{N_{site}} W_{qj} Sa_{ij}(P_k) / Sa_{ij}^{ref}(P_k). \tag{3}$$

Results

Figure 2 summarizes the results of this procedure for (200 m bins). The upper frame shows *B* as a function of depth and period. The lower frame shows basin amplification calculated by the same procedure, but replacing the spectral acceleration ratio $Sa_{ij}(P_k)/Sa_{ij}^{ref}(P_k)$ at each site by the vertically-incident plane-wave amplification factor for that site. The latter factors were computed using a plane-layered structure specific to each site, and corresponding to the SCEC-CVM shear wavespeed and density depth-profiles directly beneath that site. The main results from Figure 2 are the following: (1) Source-averaged basin amplification is period-dependent, with the highest amplifications occurring for the longest periods and greatest basin depths. (2) Relative to the very-hard rock reference structure, the maximum amplification is about a factor of 8. (3) Compared with 1D theoretical predictions, the 3D response is in most cases substantially higher. (4) The 3D response is also smoother, as a function of depth and period, than is the 1D prediction, since laterally propagating waves in the former smooth out the resonances present in the latter.

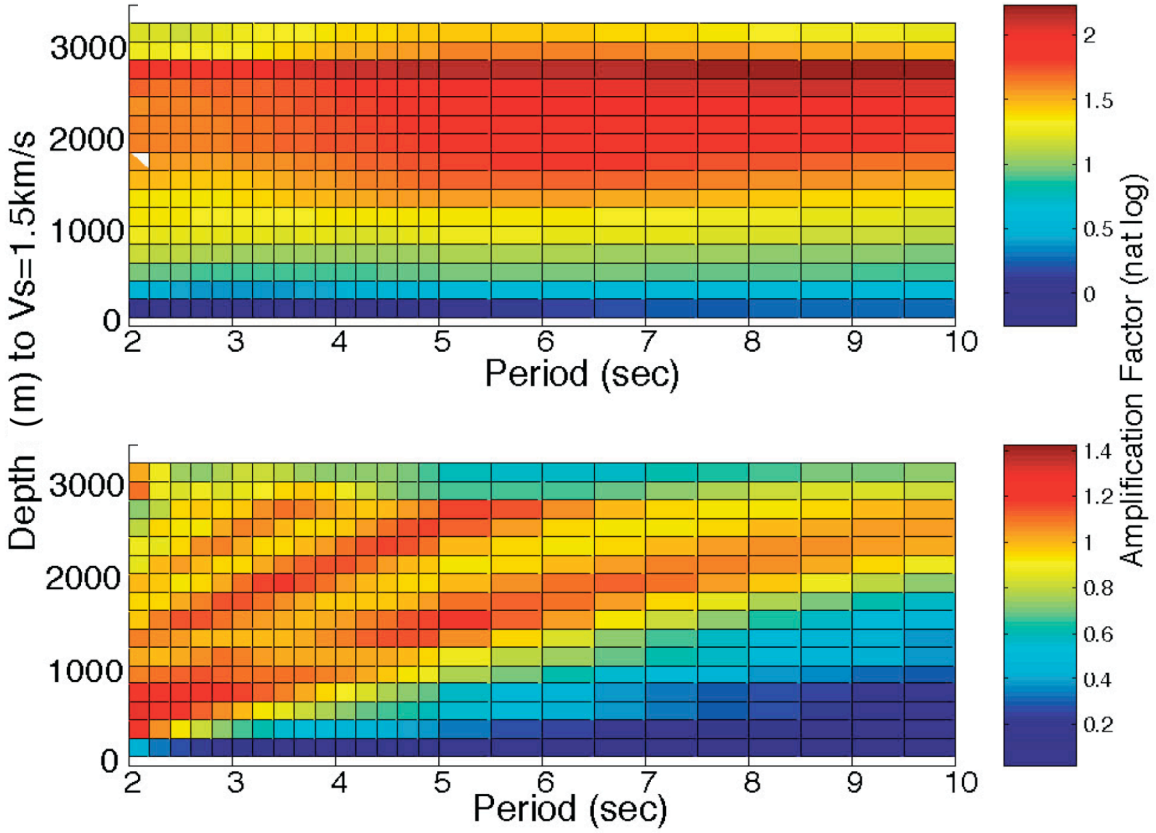

Figure 2. Top: Basin amplification versus depth and period, calculated from 3D simulations. Bottom: Basin amplification calculated by same procedure, but replacing the 3D results with 1D plane-wave amplification factors calculated using the local 1D wavespeed and density profiles (from the SCEC CVM) at each of the 1600 sites.

Figure 3 presents the results in the form of amplification curves for each of 6 periods. For depths in the range of roughly 500-1000 m, amplification decreases with period. This is, at least

qualitatively, in agreement with expectations from 1D theory: shallow sediments will have diminished effect as the wavelength becomes long relative to sediment depth. For depths exceeding about 1000 m, amplification increases with period. This is a 3D effect: higher-mode resonances present in the 1D case are smoothed out by lateral scattering, so that the longer-period resonances dominate.

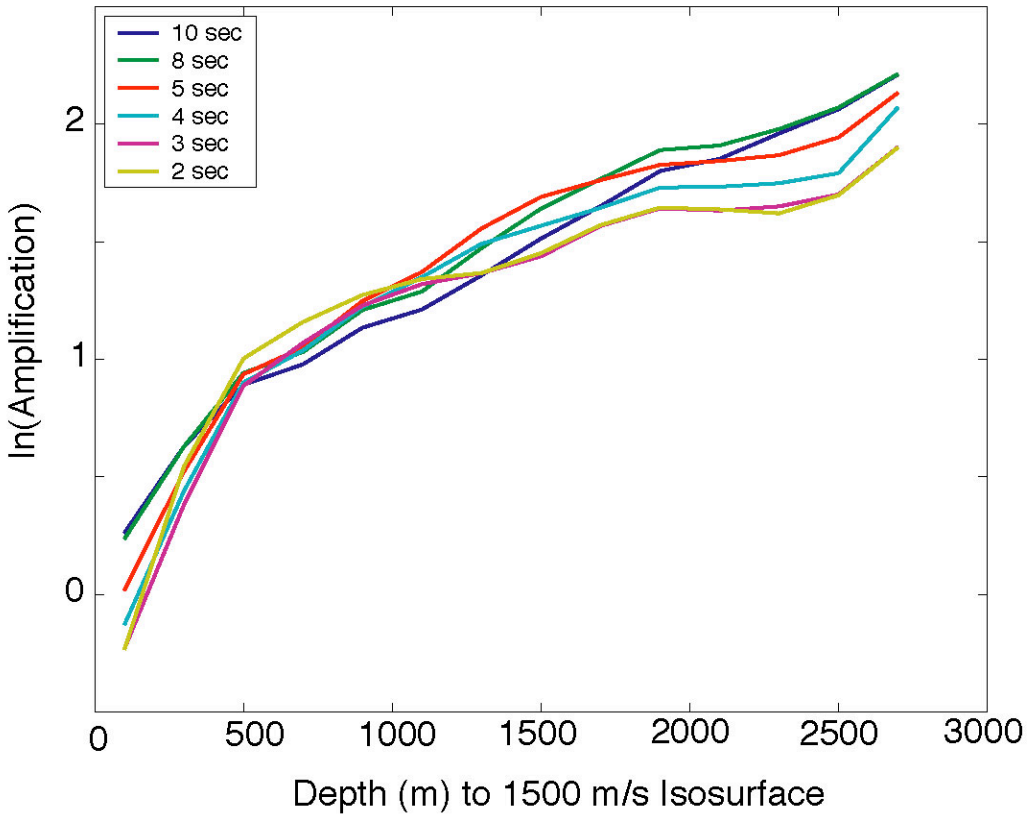

Figure 3. Basin amplification as a function of depth to 1.5 km/s *S* wave isosurface.

Parametric Model

It is useful to have a simple functional form that captures the main elements of the period- and depth-dependent basin amplification behavior observed in the simulations. One purpose of such a representation is to provide a functional form for representing basin effects in regression modeling of empirical ground motion data. We constructed a preliminary representation of this sort to provide immediate guidance to the NGA development team. Our approximate representation, $\tilde{B}(D,P)$ takes the following form:

$$\tilde{B}(D,P) = a_0(P) + a_1(P)\left[1 - \exp(D/300)\right] + a_2(P)\left[1 - \exp(D/4000)\right], \quad (4a)$$

where

$$a_i(P) = b_i + c_i P, \; i=0,1,2, \quad (4b)$$

The 6 parameters b_i, c_i were calculated in a two-step procedure. Separate least squares fits at each period P_k of $\tilde{B}(D,P_k)$ to $B(D_q,P_k)$ gave individual estimates of the $a_i(P_k)$ values for each period P_k. Then parameters b_i and c_i, for each i=0,1,2, were obtained by least-squares fitting of these 26 individual $a_i(P_k)$ estimates. The resulting values are

$$\begin{aligned} b_0 &= -1.06, \quad c_0 = 0.124, \\ b_1 &= 2.26, \quad c_1 = -0.198, \\ b_2 &= 1.04, \quad c_2 = 0.261. \end{aligned} \tag{4c}$$

The resulting amplification curves are shown in Figure 4. These expressions, despite their simplicity, represent the mean predictions of the numerical simulations quite well, and can serve as a starting point for modeling basin effects in empirical studies. In particular, they provide, in simple form, a physical basis for extrapolation of empirical models to periods greater than 2 or 3 seconds, where reliable data on basin effects are extremely scarce.

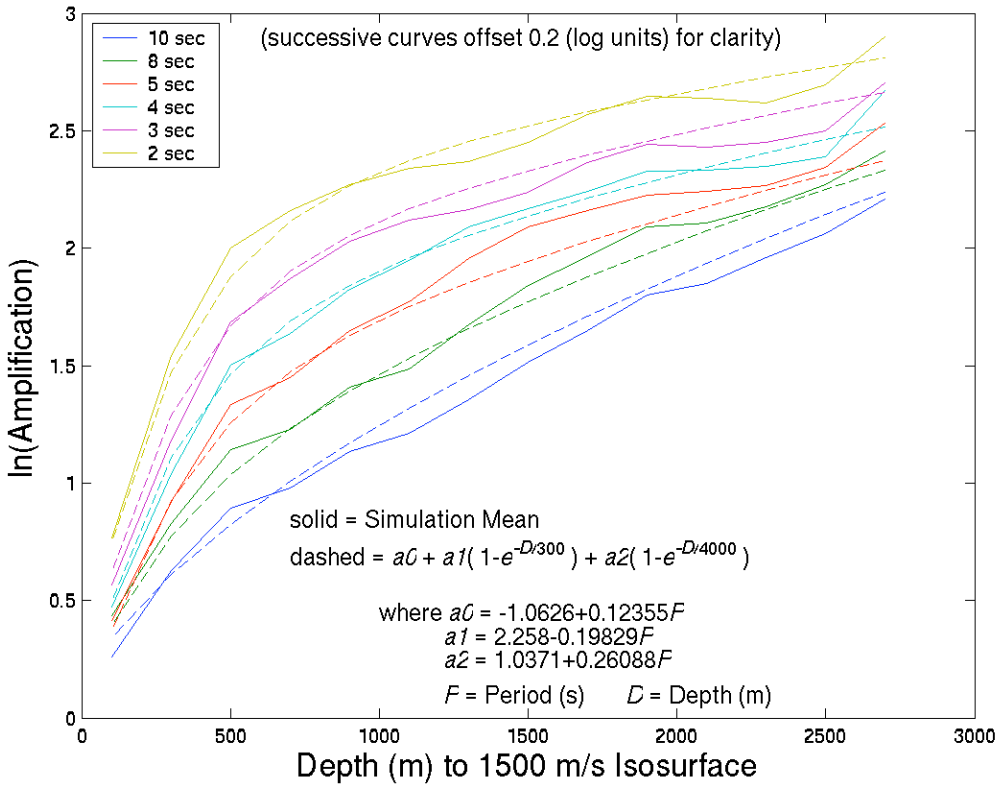

Figure 4. Parametric model $\tilde{B}$ (dashed curves) fit to basin amplification curves B (solid curves) derived by averaging 3D simulations.

Figure 5 shows the root mean square residual of $Sa_{ij}(P)/Sa_{ij}^{ref}(P)$, relative to $\tilde{B}(D,P)$, as a function of period. That is, the figure depicts R, where

$$\mathrm{R}^2\left(P_k\right)=\left(N_{ev}\sum_{j=1}^{N_{site}}W_{qj}\right)^{-1}\sum_{i=1}^{N_{ev}}\sum_{j=1}^{N_{site}}\left[Sa_{ij}(P_k)\Big/Sa_{ij}^{ref}(P_k)-\tilde{B}\left(D_j,P_k\right)\right]^2. \qquad (5)$$

The residuals decrease systematically with period. This period-dependence is what one would expect on the basis of simple physical arguments. Short-period waves are subject to short-wavelength variations due to local focusing and interference effects. Very long-period waves, in contrast, represent oscillations that are coherent over large scale lengths and are influenced principally by large-scale averages of the seismic velocity structure.

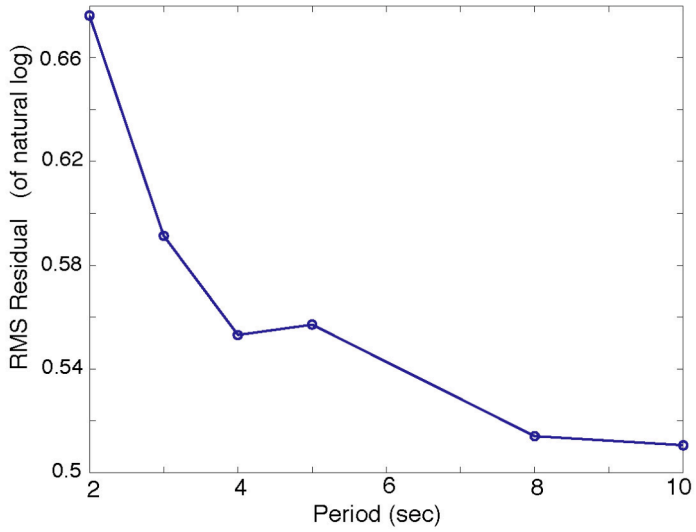

Figure 5. Root-mean-square residual of spectral acceleration amplification, relative to predictions from parametric model.

Discussion and Conclusions

We characterize the source-averaged effect of basin depth on spectral acceleration using depth (*D*) to the 1.5 km/s *S* velocity isosurface as the predictor variable. The resulting mean basin-depth effect is period dependent, and both smoother (as a function of period and depth) and higher in amplitude than predictions from local 1D models. For example, relative to a reference hard-rock site, sites with *D* equal to 2.5 km (corresponding to some of the deeper L.A. basin locations) have a predicted mean amplification factor of approximately 5.5 at 2 s period, and approximately 7.5 at 10 s period.

The basin amplification estimates described in this report are intended to guide the design of functional forms for use in attenuation relationships for elastic response spectra. In particular, they should be useful guides for extrapolating the period-dependence of basin terms to periods longer than a few seconds, where empirical data provide little constraint. More direct, quantitative use of the results may become possible in the future, however. The main requirement is that we first carefully assess the extent to which the basin effect, as defined and quantified in this study, is already accounted for implicitly in existing attenuation relationships, through (1) departures of the average "rock" site from our idealized reference model, and (2) correlation of basin depth with other predictor variables (such as Vs_{30}). A preliminary assessment

of the reference model bias is presented in Day et al. (2005). They find that the reference-model simulations under-predict the rock regression model of Abrahamson and Silva (1997) by a factor of 2 at long period (5 seconds). They argue that at the long periods considered, both source details and Vs_{30} will have minimal effects, and that this factor of 2 is likely representative of a seismic velocity shift (between the average engineering rock-site and the reference model) extending to depths of the order of half a kilometer or more. The correlation of basin effects with Vs_{30} is discussed by Choi et al. (2005), who propose data analysis procedures for separating these effects.

Acknowledgments

This work was supported by Pacific Earthquake Engineering Research (PEER) Center Lifelines Program (Tasks 1A01, 1A02, and 1A03), the National Science Foundation under the Southern California Earthquake Center (SCEC) Community Modeling Environment Project (grant EAR-0122464), and by SCEC. SCEC is funded by NSF Cooperative Agreement EAR-0106924 and USGS Cooperative Agreement 02HQAG0008.

References

Abrahamson, N. A., and W. J. Silva (1997). Empirical response spectral attenuation relations for shallow crustal earthquakes, *Seism. Res. Lett.* 68, 94-127.

Aki, K., and P. G. Richards (1980). *Quantitative Seismology, Theory and Methods*, W. H. Freeman and Co., New York.

Choi, Y., J. P. Stewart. And R. W. Graves (2005). Empirical model for basin effects accounts for basin depth and source location, Bull. Seism. Soc. Am., Vol. 95, 1412-1427, doi: 10.1785/0120040208.

Day, S. M., J. Bielak, D. Dreger, R. Graves, S. Larsen, K. Olsen, and A. Pitarka (2001). *Tests of 3D elastodynamic codes: Final report for Lifelines Project 1A01*, Pacific Earthquake Engineering Research Center.

Day, S. M., J. Bielak, D. Dreger, R. Graves, S. Larsen, K. Olsen, and A. Pitarka (2003). *Tests of 3D elastodynamic codes: Final report for Lifelines Project 1A02*, Pacific Earthquake Engineering Research Center.

Day, S. M., J. Bielak, D. Dreger, R. Graves, S. Larsen, K. Olsen, and A. Pitarka (2005). 3D ground motion simulation in basins*: Final report for Lifelines Project 1A03*, Pacific Earthquake Engineering Research Center.

Magistrale, H., S. M. Day, R. Clayton, and R. W. Graves (2000). The SCEC southern California reference three-dimensional seismic velocity model version 2, *Bull. Seism. Soc. Am., 90*, S65-S76.

Olsen, K. B., S. M. Day, and C. R. Bradley (2003). Estimation of Q for long-period (>2 s) waves in the Los Angeles Basin, *Bull. Seism. Soc. Am.*, *93*, 627-638.

Somerville, P.G., K. Irikura, R. Graves, S. Sawada, D. Wald, N. Abrahamson, Y. Iwasaki, T. Kagawa, N. Smith and A. Kowada (1999). Characterizing crustal earthquake slip models for the prediction of strong ground motion, *Seism. Res. Lett. 70,* 59-80.